Visuospatial Working Memory under Fatigue: Observations with Cerebral Hemodynamics and Heart Rate Variability

Visuospatial working memory (WM) is a central component of human executive function within safety-critical systems, where the interactions between fatigue due to time-on-task and WM capacity remain critical yet under-explored dimensions. In this work, we investigate the temporal dynamics of brain activation, functional connectivity, and heart-rate variability (HRV) during a fatiguing visuospatial two-back test. We recruited sixteen participants who were subject to this protocol while we captured their neurophysiological data through near-infrared spectroscopy and HRV. We observed that brain activation in the pre-frontal cortex (PFC) mirrors performance, where, with the onset of fatigue we found a decrease in both measures. Functional connectivity strengths were found to decrease between key PFC regions and the secondary visual cortex suggesting fatigue-induced task disengagement. Further, we explored the validity of the neurovisceral integration model in explaining HRV changes against brain activation. Together, our observations support the development of a predictive framework for WM decline.

Introduction

Working memory (WM) is a neurological process where the brain temporarily stores and manipulates information in order to perform cognitive functions such as, learning, language comprehension, and reasoning (Baddeley, 2000). The brain relies on a complex network of resources to facilitate these processes, and associated executive functions (Owens, Duda, Sweet, & MacKillop, 2018). WM and sustained attention remain a central component to effective job performance in domains such as emergency response, front-line medical practice, and air-traffic control, where personnel are required to exhibit high levels of comprehension, reasoning, and vigilance for extended periods (Causse, Dehais, & Pastor, 2011). In these safety-critical systems, executive functions are often compromised by cognitive fatigue due to lapses in working conditions, the nature of the job, long work hours or a combination of related factors.

Fatigue induces additional cognitive burden, which can impair WM and limit our ability to sustain task demands. For example, physicians when multitasking or interrupted were prone to misdiagnoses, and when sleep deprived their error rates increased by more than 15 times the nominal value (Westbrook, Raban, Walter, & Douglas, 2018). In another example, wildland firefighters were reportedly sleep deprived by up to 35 hours each week during stretches of the peak fire season, which severely degrades their situation awareness and decision-making capabilities (Vincent et al., 2018). Therefore, the need to study the interplay between fatigue and WM capacity is not understated.

Previous studies have explored the neural underpinnings of WM (Gazzaley, Rissman, & D'esposito, 2004), and its sensitivity to cognitive fatigue (Marshall, Forstot, Callies, Peterson, & Schenck, 1997) with varying levels of success. For example, (Sun et al., 2019) demonstrated that functional connectivity and causality analyses during a short duration (less than 10 minutes) n-back test were more informative of changes in WM performance than other measures. In another study, (Dehais et al., 2018) found that brain-based metrics using functional near-infrared spectroscopy (fNIRS) could successfully classify workload during a working memory task within a flight training simulator. However, neuroimaging tools available today remain cumbersome for most real-world applications.

The neurovisceral integration model (NVIM) proposed by Thayer et al., provides a framework to juxtapose vagal activity, prefrontal cortex (PFC) activation, and executive function (Thayer & Lane, 2000). Vagal activity can serve as a useful analogue to neural data while relying on unobtrsuive sensing instruments. Specifically, they provide evidence to suggest that the primary role of the PFC during a WM task is in sensory inhibition, where with increased PFC activity we expect an increase in parasympathetic tone, and therefore an increase in heart rate variability (HRV) (Thayer, Hansen, Saus-Rose, & Johnsen, 2009). However, study designs, and findings remain variable, with conflicting observations on the relationship between HRV indices and WM demand. For example, in a recent study, Condy et al. extended the NVIM to explore comparisons between neural activity and HRV during a response inhibition task, where they found that baseline HRV agreed with NVIM expectations, but trends during active inhibition were mostly inconsistent (Condy, Friedman, & Gandjbakhche, 2020). This reasserts the need for further exploration on task-specificity and environmental demands to assess the relevance of the NVIM franework. Addressing gaps in this space remains critical towards the development of robust state estimation methods free from the practical encumbrances of current neuroimaging tools.

To that end, this study is centered on understanding WM capacity under the influence of fatigue using neural and physiological indices. We approach this problem by employing a protracted version of a visuospatial (VS) two-back test which demands high WM under constant workload, and high sustained attention given the time-on-task. The primary aim was to examine the spatio-temporal dynamics of neural activity, and the temporal dynamics of physiological response during this fatiguing VS WM task. A secondary aim was to compare neurophysiological signal behaviors to expectations from the NVIM framework. Together, fNIRS

and HRV based indices enable advances toward a robust predictive framework for recognizing WM deficits in the wild.

Materials and Methods

Experiment

Participants. Sixteen participants were recruited (Age: 25.12 ± 3.31 years; 8 female) from the local student population. Only nine among them produced neural data compatible for subsequent analyses, among who, five were female. All participants were right-hand dominant, and provided informed consent before the start of the experiment protocol. All experimental procedures were approved by the university's Institutional Review Board, and proceeded in accordance with the *Ethics Code* of the *American Psychological Association*.

Protocol. Upon informed consent, participants were equipped with relevant bio-instruments and responded to questionnaires on their demographics, sleepiness (Karolinska Sleepiness Scale, (Kaida et al., 2006)) and mood (Profile of mood states, (Shacham, 1983)). Participants were then instructed to rest for five minutes with their eyes closed in a seated position to capture a baseline across all sensing instruments. They were then introduced to the VS WM task which included a training period followed by the actual experiments. The task consisted of 12 blocks, with each block lasting a duration of five minutes. Between blocks participants responded to single-element questionnaires on their fatigue, effort, and discomfort. On completing the 12 block protocol participants again responded to subjective sleepiness and mood assessments. The complete protocol is shown in **Fig. 1 (a)**.

Visuospatial working memory task. The WM task employed in this study was a VS two-back test. The task was presented on a static web page where participants tracked a green circle within a 3×3 grid. The circle would appear in different sections of the grid; if the first position of the circle matched the one from two steps ago, then participants would respond with a key-press. The inter-stimulus time was $1000ms$, and the image persistence time was $900ms$. The match probability was set to 0.5, where the interface provided a fixed, temporally randomized number of match events in each block (N = 94; see **Fig. 1(b)**). Before participants began the experiment, they were allowed to practice the two-back task under a training mode. The training interface provided feedback on response correctness and response time. During the experiment, this feedback was withheld from participants. The interface recorded every key-press or lapse event on the task with time stamps and a response correctness flag (hit, miss or false-alarm). For subsequent discussions in this article, the performance measure used was the overall accuracy on the task.

Bioinstruments. Participants wore a continuous wave functional near-infrared spectroscopy (fNIRS) device (NIRSport2, NIRx Medical Technologies LLC, USA). Cortical hemodynamics was obtained using the fNIRS device at $50Hz$. Near infrared spectra were captured at two wavelengths ($\lambda = 760$ & $850nm$). There were a total of 16 infrared

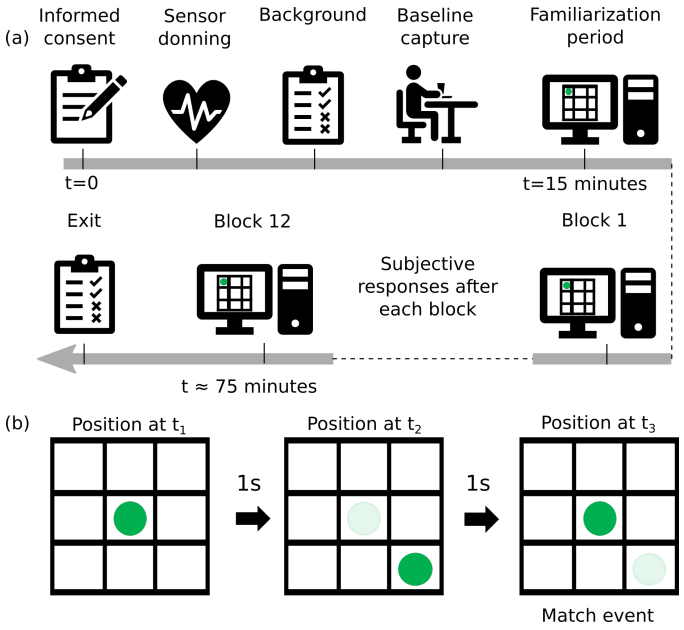

Fig. 1. (a) Schematic representation of the experiment protocol and timeline. (b) Representation of a two-back match event when the user is expected to respond with a key-press.

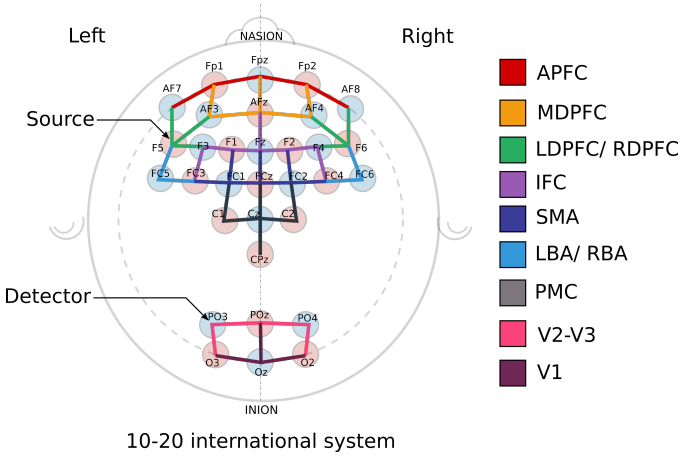

Fig. 2. Schematic representation of the probe-map used for neuroimaging via functional near-infrared spectroscopy (fNIRS). The probe-map consisted of eleven regions of interest derived from the 10-20 EEG system, here the red circles represent IR sources, and the blue circles depict the IR detectors.

(IR) sources and 16 IR detectors that characterized blood distribution about the brain across 46 channels. Channels were focused on 11 regions: anterior prefrontal cortex (APFC), medial dorsolateral PFC (MDLPFC), right (R) DLPFC, left (L) DLPFC, intermediate frontal cortex (IFC), right Broca's area (RBA), left Broca's area (LBA), premotor cortex (PMC), supplementary motor area (SMA), secondary and tertiary visual cortex (V2-V3), and the primary visual cortex (V1; see complete probe-map in **Fig. 2**). In addition to the fNIRS device, participants were instrumented with an electrocardiography (ECG) device (Actiheart 4, CamNTech, Inc., UK) that was used to collect ECG data at $128Hz$. Electrodes were placed at the base of the sternum and just beneath the left

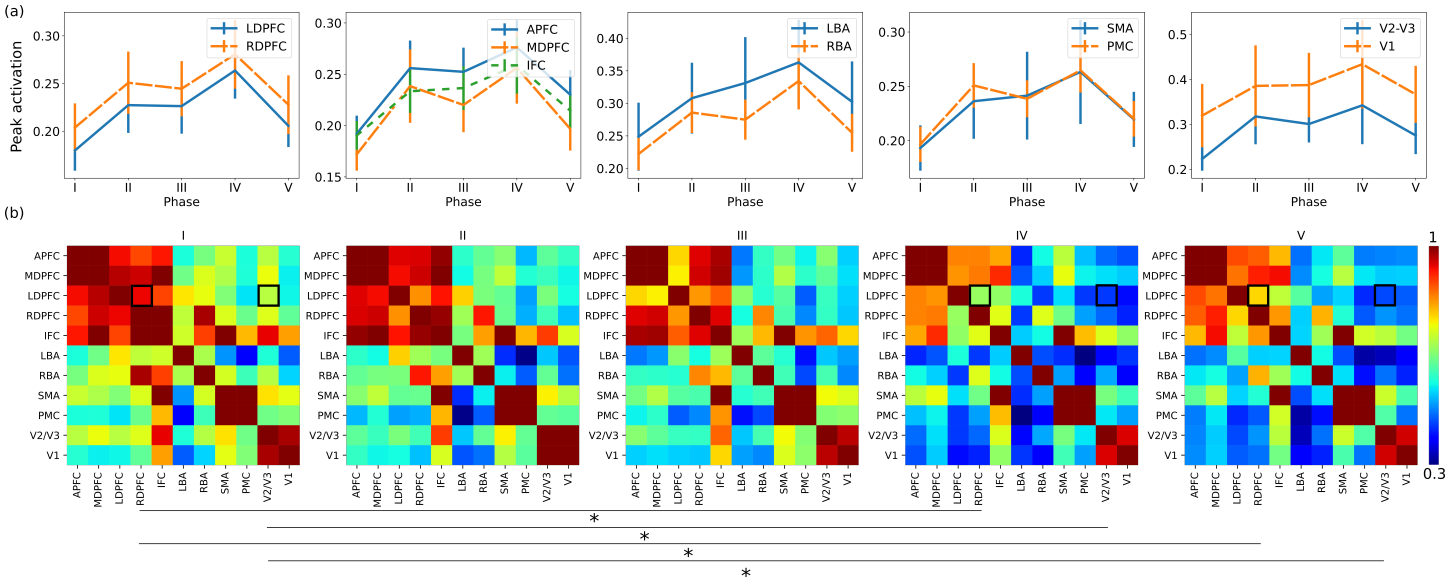

Fig. 3. (a) Peak activation across the 11 brain regions are shown in the form of line graphs with S.E.M at each time-point. Results from the one-way RMANOVA revealed a significant effect of time in eight out of eleven regions. (b) Functional connectivity (FC) differences across each time point. The graphic presents the the normalized mean z-score of FC by ROI across all participants at each time point. Pairwise t-tests revealed significant differences in FC across LDPFC-RDPFC regions across phases I-IV, and I-V. Similar differences were observed across the LDPFC and V2-V3 regions.

pectoralis minor muscle.

Pre-processing and feature extraction

fNIRS. Light intensity recorded from the fNIRS device was first converted to optical density. The optical density signal was low-pass filtered to attenuate high frequency noise. Motion artifacts were removed through peak detection and spline interpolation. The smoothed signals were band-pass filtered to reduce the effect of slow wave drifts and physiological noise in the data. Lastly, the change in oxygenated, deoxygenated, and total hemoglobin concentration (ΔHbO/R/T) was derived using the modified Beer-Lambert principle with a processing stream consistent with (Nuamah, Mantooth, Karthikeyan, Mehta, & Ryu, 2019). For the scope of the analyses presented in this article we relied on the ΔHbO data which was used to derive channel-wise functional connectivity (FC) metrics and peak activation. The raw time-series ΔHbO was sampled with a window of duration $15s$ which accommodates the underlying periodicity of the hemodynamic response. The peak values and FC measures were derived across each window for subsequent analyses. For FC measures we relied on Pearson's correlation coefficients that were transformed using Fisher's method (Rhee & Mehta, 2018).

Heart rate variability. The raw ECG signal was filtered for motion-related artifacts (Strasser, Muma, & Zoubir, 2012), and corrected for ectopics with polynomial interpolation (Marked, 1995). Subsequently, a peak detection algorithm was used to isolate the R peaks from the ECG signal (Li, Zheng, & Tai, 1995). The time between successive R-R peaks, i.e. the inter-beat-interval ($\mathbf{X}_{IBI}$) or normal-to-normal (NN) interval was then derived from the processed peak signals. We derived four representative statistics for statistical analyses, two in the time domain (standard deviation of NN interval ($sdnn$), and root mean squared of successive differences ($rmssd$)), and two in the frequency domain (low-frequency (lf) and high frequency (hf) power), these features were chosen given prior evidence of their relevance within the NVIM.

Statistical analysis

Blocking. The fNIRS data, HR/V features, and performance measure were blocked into five phases – *I, II, III, IV*, and *V*; where each variable was characterized by its block mean. Each phase consisted of two experiment blocks for phase *I* to *IV*, while phase *V* was made up of three blocks. Each block lasted a duration of five minutes, with $\approx 30s$ of transition time between them, where participants respond to a single-element subjective questionnaire. The last block (no. 12) was dropped from our analyses due to a self-reported anticipatory effect for experiment completion.

Methods. The performance measure was not normally distributed, therefore we relied on the Friedman's test, a non-parametric equivalent to the one-way repeated measures analysis of variance (ANOVA) to assess the main effect of time. Kendall's W was used as an estimate for effect size on the Friedman's test, with Wilcoxon signed-rank tests for post-hoc analyses. On the fNIRS data, a one-way repeated measures ANOVA was applied to assess the main effect of time (five phases) on peak activation for each region. Multiple pairwise paired t-tests were used to assess the significance between the levels of the within subjects factor (time). Functional connectivity data was subject to simple paired t-tests to identify significantly different FC pairs across each time point. HR/V measures were blocked similar to FC and peak activation data, and subject to a one-way repeated measures ANOVA. *Bonferroni* adjusted *p-values* were used as a threshold to determine significance

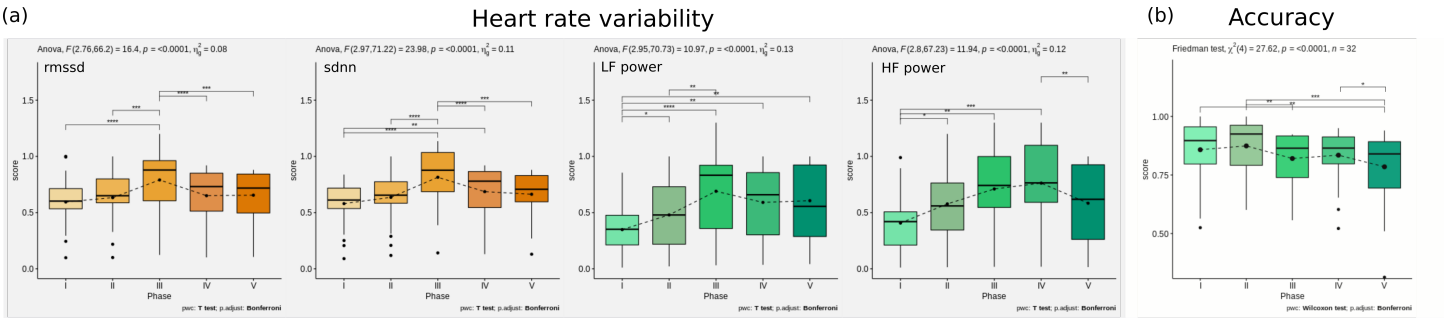

Fig. 4. (a) Results from the one-way repeated measures ANOVA on the HR/V features. A significant effect of time was observed across all measures with a small to moderate effect size. (i) Time domain features – RMSSD, and SDNN. (ii) Frequency domain features – spectral power densities in the LF and HF regimes. (b) Results from the non-parametric Friedman's test for the overall performance accuracy across the five phases.

where relevant. For purposes of clarity, data in the figures are illustrated using standard error of the mean (S.E.M.)

Results

Peak activation

A significant main effect of time was found on peak activation across the APFC, LDPFC, MDPFC, RDPFC, RBA, PMC, IFC, and LBA regions (all $p < 0.036$, $\eta_g^2 \in [0.08 - 0.15]$). This significance was not observed for the V1, V2/V3 or SMA regions (all $p > 0.075$). **Fig. 3 (a)** presents the peak activation trends across all regions. Post-hoc, pairwise comparisons revealed a consistent pattern of temporal difference in the APFC, LDPFC, MDPFC, RDPFC, and RBA regions, where we observe an increase in peak activation going from phase *I* to phases *II*, *III*, and *IV* respectively; no significant differences were seen between phases *II*, *III* and *IV*, and a decrease in peak activation was observed from phase *IV* to *V* of the experiment. In the LBA, PMC, and IFC regions the peak differences between the phase *I* and phases *II*, *III* and *IV* persisted, but no decrease in activation was observed going from phase *IV* to *V*.

Functional connectivity

Fig. 3 (b) presents the normalized mean z-score of FC across all region-pairs at each time point. From our analyses we observe that **(i)** network-wide FC is positive, and **(ii)** a global decrease in functional connectivity is apparent from phase *I* to *V*. Although global changes are visually apparent for the mean value, given variability in FC response, only a few region-time point pairs exhibit a statistically significant decrease in FC values. These were (as highlighted), LDPFC - RDPFC associations between phase pairs *I* to *IV* and *I* to *V* ($p = 0.041, 0.032$ respectively); and LDPFC - V2/V3 between *I* to *IV* and *I* to *V* ($p = 0.046, 0.036$ respectively).

Heart rate variability

A significant main effect of time was found across all four HRV measures (all $p < 0.0001, \eta_g^2 \in [0.08 - 0.13]$; **Fig. 4 (a)**). For the LF measure, post-hoc comparisons revealed significant differences in the mean values between phase *I*, and all other subsequent phases. Notably, we found that LF power density increases relative to phase *I* in all other subsequent phases. A similar increase was found going from phase *II* to *III*; notably this difference is not present between phases *III*, *IV*, and *V*, where the measure appears to have plateaued. On HF a significant increase was evident between phase *I* and phases *II*, *III*, and *IV* respectively, a similar increase was also seen between phases *IV*, and *V*; no other pairs were found significant. Across the time domain features, for SDNN and RMSSD we observed significant increases across phase pairs *I* to *III*, and *II* to *III*, while, a decrease was observed between phase pairs *III* to *IV*, and *IV* to *V* respectively.

Performance accuracy

A main effect of time was found on the performance accuracy metric ($p < 0.0001, K_w = 0.21$). Post-hoc analyses revealed a marginal increase in accuracy going from phase *I* to phase *II*, a decrease in accuracy from phase *II* to phase *III*, and a further decrease in accuracy levels from phase *IV* to phase *V* (all $p < 0.042$).

Discussion

The primary role of the frontal cortex during working memory tasks such as the one discussed in this study is towards sensory inhibition, i.e. reducing the influence of distracting streams of information to retain focus on task goals. Therefore, an increase in PFC activity would be indicative of the effort employed by the participants in doing well on the WM task. Clearly, early trends in prefrontal activity supports this argument, where we saw an increase in peak activation from phase *I* until phase *IV*. Performance adds more context to this discussion, where we observed that there is a distinct learning period with improvements in task performance. This ''learning'' was characterized by an increase in overall accuracy from phase *I* to *II* which was concomitant with increases in neural activation. Beyond phase *II*, the observations take on an interesting turn, where we found that performance accuracy plateaus across phases *II*, *III* and *IV*, while neural activity increased – this is characteristic of increasing effort and the brain recruiting additional resources to meet task workload demands, while performance itself appears to have saturated (Causse, Chua,

Peysakhovich, Del Campo, & Matton, 2017). Moreover, during this period we also discovered an increase in neural activity across regions peripheral to the PFC including, the IFC, LBA, RBA, and PMC regions, which further supports the preceding argument. Finally, across phases *IV* and *V*, we observed a decrease in overall accuracy that was mirrored by a decrease in activity in the LDPFC, a region most often touted as responsible for WM capacity (Barbey, Koenigs, & Grafman, 2013). This decrease in LDPFC activation was accompanied by a plateau in other brain regions, which leads-in to our discussion on the influence of fatigue on working memory capacity.

We found that with prolonged time on task, participants reported greater fatigue and this was associated with diminished cognitive capacity to sustain inhibitory control (i.e., lower accuracies). This was also evident from a global decrease in peak activation across all PFC regions going from phase *III* to phase *V*. Functional connectivity analyses found declines in connectivity strengths across two regions, namely, the LDPFC-RDPFC and the LDPFC-V2/V3 regions. In particular, the decline in connectivity between LDPFC and RDPFC highlights the neural underpinnings of the impact of fatigue on WM and the decline in LDPFC-V2/V3 connectivity supports our hypothesis that, with time-on-task participants are driven towards (visual) disengagement under fatiguing conditions (Gazzaley et al., 2004).

The NVIM offers a framework to connect changes in PFC activation to parasympathetic activity and HRV. We observed a clear increase in HRV as indexed by RMSSD, and SDNN from phase *I* to phase *III*, this aligns with the perspective that, as PFC activity increased, heart rate decreases and in turn we observe an increase in the temporal characteristics of HRV. This argument is further substantiated by observations in the spectral domain, where we found that the LF power density mirrors these time-domain trends. This finding is bolstered by the idea that as PFC activity (or sensory inhibition) increases, we expect an increase in vagal activity which is empirically associated with LF power under controlled conditions (Thayer et al., 2009). These observations are unique and promising, especially given that temporal dynamics of HRV agree with NVIM-driven expectations and shadow the neural source while under fatigue. This is a key piece of the puzzle in our pursuit of unobtrusive sensing paradigms for robust and prescient state recognition. For example, the recognition of working memory deficits in emergency responders may benefit from technologies that rely on cognitive capacities that demonstrate such underlying neurophysiological dynamics. To that end, future work may need to address study limitations, such as, (i) expanding the sample size that supports these observations, (ii) investigating causality to determine patterns in network connectivity changes, and (iii) improving the relevance of experimental paradigms towards applications in emergency response.

REFERENCES

Baddeley, A. (2000). The episodic buffer: a new component of working memory? *Trends in cognitive sciences*, *4*(11), 417–423.

Barbey, A. K., Koenigs, M., & Grafman, J. (2013). Dorsolateral prefrontal contributions to human working memory. *cortex*, *49*(5), 1195–1205.

Causse, M., Chua, Z., Peysakhovich, V., Del Campo, N., & Matton, N. (2017). Mental workload and neural efficiency quantified in the prefrontal cortex using fnirs. *Scientific reports*, *7*(1), 1–15.

Causse, M., Dehais, F., & Pastor, J. (2011). Executive functions and pilot characteristics predict flight simulator performance in general aviation pilots. *The International Journal of Aviation Psychology*, *21*(3), 217–234.

Condy, E. E., Friedman, B. H., & Gandjbakhche, A. (2020). Probing neurovisceral integration via functional near-infrared spectroscopy and heart rate variability. *Frontiers in Neuroscience*, *14*.

Dehais, F., Dupres, A., Di Flumeri, G., Verdiere, K., Borghini, G., Babiloni, F., & Roy, R. (2018). Monitoring pilot's cognitive fatigue with engagement features in simulated and actual flight conditions using an hybrid fnirs-eeg passive bci. In *2018 ieee international conference on systems, man, and cybernetics (smc)* (pp. 544–549).

Gazzaley, A., Rissman, J., & D'esposito, M. (2004). Functional connectivity during working memory maintenance. *Cognitive, Affective, & Behavioral Neuroscience*, *4*(4), 580–599.

Kaida, K., Takahashi, M., Åkerstedt, T., Nakata, A., Otsuka, Y., Haratani, T., & Fukasawa, K. (2006). Validation of the karolinska sleepiness scale against performance and eeg variables. *Clinical neurophysiology*, *117*(7), 1574–1581.

Li, C., Zheng, C., & Tai, C. (1995). Detection of ecg characteristic points using wavelet transforms. *IEEE Transactions on biomedical Engineering*, *42*(1), 21–28.

Marked, V. (1995). Correction of the heart rate variability signal for ectopics and missing beats. *Heart rate variability*.

Marshall, P. S., Forstot, M., Callies, A., Peterson, P. K., & Schenck, C. H. (1997). Cognitive slowing and working memory difficulties in chronic fatigue syndrome. *Psychosomatic Medicine*, *59*(1), 58–66.

Nuamah, J. K., Mantooth, W., Karthikeyan, R., Mehta, R. K., & Ryu, S. C. (2019). Neural efficiency of human–robotic feedback modalities under stress differs with gender. *Frontiers in human neuroscience*, *13*, 287.

Owens, M. M., Duda, B., Sweet, L. H., & MacKillop, J. (2018). Distinct functional and structural neural underpinnings of working memory. *NeuroImage*, *174*, 463–471.

Rhee, J., & Mehta, R. K. (2018). Functional connectivity during handgrip motor fatigue in older adults is obesity and sex-specific. *Frontiers in human neuroscience*, *12*, 455.

Shacham, S. (1983). A shortened version of the profile of mood states. *Journal of personality assessment*.

Strasser, F., Muma, M., & Zoubir, A. M. (2012). Motion artifact removal in ecg signals using multi-resolution thresholding. In *2012 proceedings of the 20th european signal processing conference (eusipco)* (pp. 899–903).

Sun, J., Liu, F., Wang, H., Yang, A., Gao, C., Li, Z., & Li, X. (2019). Connectivity properties in the prefrontal cortex during working memory: a near-infrared spectroscopy study. *Journal of biomedical optics*, *24*(5), 051410.

Thayer, J. F., Hansen, A. L., Saus-Rose, E., & Johnsen, B. H. (2009). Heart rate variability, prefrontal neural function, and cognitive performance: the neurovisceral integration perspective on self-regulation, adaptation, and health. *Annals of Behavioral Medicine*, *37*(2), 141–153.

Thayer, J. F., & Lane, R. D. (2000). A model of neurovisceral integration in emotion regulation and dysregulation. *Journal of affective disorders*, *61*(3), 201–216.

Vincent, G. E., Aisbett, B., Wolkow, A., Jay, S. M., Ridgers, N. D., & Ferguson, S. A. (2018). Sleep in wildland firefighters: what do we know and why does it matter? *International journal of wildland fire*, *27*(2), 73–84.

Westbrook, J. I., Raban, M. Z., Walter, S. R., & Douglas, H. (2018). Task errors by emergency physicians are associated with interruptions, multitasking, fatigue and working memory capacity: a prospective, direct observation study. *BMJ quality & safety*, *27*(8), 655–663.